

Review

# Orthopedics-Related Applications of Ultrafast Laser and Its Recent Advances

Celina L. Li <sup>1,\*</sup> , Carl J. Fisher <sup>1</sup>, Ray Burke <sup>1</sup> and Stefan Andersson-Engels <sup>1,2,\*</sup>

<sup>1</sup> Biophotonics@Tyndall, IPIC, Tyndall National Institute, Lee Maltings, Dyke Parade, T12 R5CP Cork, Ireland; carl.fisher@tyndall.ie (C.J.F.); ray.burke@tyndall.ie (R.B.)

<sup>2</sup> Department of Physics, University College Cork, T12 R5CP Cork, Ireland

\* Correspondence: liyao.li@tyndall.ie (C.L.L.); stefan.andersson-engels@tyndall.ie (S.A.-E.);

Tel.: +353-(0)21-2346946 (C.L.L.); +353-(0)21-2346118 (S.A.-E.)

**Abstract:** The potential of ultrafast lasers (pico- to femtosecond) in orthopedics-related procedures has been studied extensively for clinical adoption. As compared to conventional laser systems with continuous wave or longer wave pulse, ultrafast lasers provide advantages such as higher precision and minimal collateral thermal damages. Translation to surgical applications in the clinic has been restrained by limitations of material removal rate and pulse average power, whereas the use in surface texturing of implants has become more refined to greatly improve bioactivation and osteointegration within bone matrices. With recent advances, we review the advantages and limitations of ultrafast lasers, specifically in orthopedic bone ablation as well as bone implant laser texturing, and consider the difficulties encountered within orthopedic surgical applications where ultrafast lasers could provide a benefit. We conclude by proposing our perspectives on applications where ultrafast lasers could be of advantage, specifically due to the non-thermal nature of ablation and control of cutting.

**Keywords:** ultrafast lasers; laser ablation; orthopedic surgery; clinical translation; surface modification



**Citation:** Li, C.L.; Fisher, C.J.;

Burke, R.; Andersson-Engels, S.

Orthopedics-Related Applications of

Ultrafast Laser and Its Recent

Advances. *Appl. Sci.* **2022**, *12*, 3957.

<https://doi.org/10.3390/app12083957>

Academic Editor: Christian Spielmann

Received: 24 March 2022

Accepted: 11 April 2022

Published: 14 April 2022

**Publisher's Note:** MDPI stays neutral with regard to jurisdictional claims in published maps and institutional affiliations.



**Copyright:** © 2022 by the authors. Licensee MDPI, Basel, Switzerland. This article is an open access article distributed under the terms and conditions of the Creative Commons Attribution (CC BY) license (<https://creativecommons.org/licenses/by/4.0/>).

## 1. Introduction

Lasers have been applied in many fields of medicine to treat diseases since invented. Today, there is a rapidly growing interest in the use of lasers in orthopedic procedures such as osteotomy [1–3], oral [4–6] and spine [7,8] surgeries, as well as in cellular biology [9] and material micromachining [10]. Ultrafast laser, namely pulse widths of nominally a few picoseconds (ps) or shorter, has notably attracted considerable attention due to its unique property of optical nonlinearities. A wide range of applications has since been adapted in biophotonics such as multiphoton microscopy, cataract surgery and cell molecular manipulations [11]. In dentistry, the use of ultrafast lasers has proven promising for developing surgical procedures with higher precision and improved outcomes [12–15]. Even though a tremendous amount of research has gone into the field, a search of “ultrafast laser”, “orthopedics” and “bone” yielded no review articles at the time of writing, specifically examining orthopedic applications using ultrafast lasers. We therefore surveyed the literature and considered the following questions: (1) With recent advances, is ultrafast laser technology matured enough for clinical dissemination for uses in orthopedic surgeries and what are some still existing barriers? (2) What is the current status in orthopedic bone repair and implants? (3) What are some potential future studies and perspectives for ultrafast lasers in the field of orthopedics? The aim of this review is to provide an overview of recent advances in orthopedics-related applications using ultrafast lasers with the primary focus on bone ablation and implant processing, in an effort to critically evaluate new progress and provide some insights in the field. This paper begins with a brief background description of ultrafast lasers followed by recent studies in orthopedic surgery and bone implant processing, and lastly, perspectives on future directions.

## 2. Background

Laser ablation of bone tissue has gradually been introduced and accepted clinically as complementary techniques due to its higher precision and non-contact nature, although mechanical methods such as the use of drills, burrs, saws and milling cutters remain the gold standard for bone cutting procedures [16,17]. In particular, compared to laser ablation, mechanical instruments during bone cutting generate substantial thermal damage, bone fragmentation, amorphous formation and a mineral-rich carbon layer as well as biomechanical stress to adjacent structures; yet surgical protocols are well-established for these tools with acceptable clinical outcomes [1]. Among the many types of clinical laser systems, several common ones found within the field of orthopedics are Er:YAG, Nd:YAG, Argon and CO<sub>2</sub> lasers, which machine bone structures by the means of vaporization and melt expulsion [1,18,19] (Table 1). These conventional clinical laser systems, which have been developed often as continuous-wave or with longer wave pulse (in the  $\mu\text{s}$  and sub- $\mu\text{s}$  range), depend primarily on the linear absorption of light by the target chromophore(s); thus, the penetration depth is significantly affected by the absorption coefficient of water in an inverse relationship [1]. Due to the strong wavelength-dependent nature, non-deterministic ablation can be generated in highly heterogenous tissue structures leading to unnecessary injuries. Collateral damage surrounding the laser focal volume can also be induced by excessive heat release, thus greatly hampering bone healing and regeneration [1,16,17,20].

**Table 1.** The conventional lasers commonly used in bone-related procedures, with operation wavelengths and absorption chromophores [1,18,19].

Laser	Wavelength (nm)	Absorption Chromophore	Typical Laser Power (W)
Er:YAG	2940	Water	100–2250 [21]
Nd:YAG	1064	Pigment, proteins	43–86 [22]
Argon	514	Pigment, hemoglobin	1.5–3 [23]
CO <sub>2</sub>	10,600	Water	5–40 [24]

The potential and efficiency of ultrafast pulsed laser (pulse ranging approximately from 100 fs to 10 ps) for ablating biological hard tissues has been extensively studied to overcome the thermal and thermo-mechanical drawbacks of the conventional laser systems. In particular, an ultrafast laser source is capable of producing extremely high peak radiation intensities ( $>10^{11}$  W/cm<sup>2</sup>), leading to the initial generation of free electrons through a multiphoton absorption mechanism and band-gap (Zener) tunnelling. A high density of excited electrons is therefore created locally in a small focal volume due to nonlinear absorption, triggering avalanche ionization that supports plasma formation. Ablation of tissue is then generated by the rapidly expanding high-density plasma, forming smoother cavity walls with negligible thermal damage. This process is known as plasma-mediated ablation or laser-induced breakdown. A free electron formed during the multiphoton absorption and avalanche ionization processes can be promoted from the ground state to the valence band by the energy of two, three, four, five and six photons for wavelengths longer than 191, 383, 574, 766 and 958 nm, respectively. Wavelength dependence of the process thus indicates decreased tissue damage threshold along with decreasing wavelength [25]. Thermal damage can remain highly confined in the focal volume during optical breakdown not only because the location of plasma formation can be controlled by precise energy deposition using focused laser radiation but also because ultrafast laser pulses are a few orders of magnitude shorter than thermal diffusion time (heat transfer ranging in the order of picoseconds to nanoseconds from absorbing proteins to tissue water) [26–28]. A standard state-of-the-art ultrafast laser system normally uses a Ti:sapphire oscillator in the near-infrared region or infrared region (NIR/IR) for tissue ablation, where the pulse width and repetition rate can vary depending on the application. Interested readers can find more details on ultrafast laser interactions and mechanisms with biological hard tissues from literature reviews [20,29–34]. Advantages of using ultrafast laser over longer wave pulse laser have also been recognized, specifically including absence of melting,

carbonization or microcracks; negligible collateral damage; selective ablation with increased precision; and the potential for delivering minimal invasive procedures [35]. The inherent limitations of ultrafast laser tissue ablation lie in the penetration depth and precision, primarily because of nonlinear self-focusing, plasma defocusing and normal group velocity dispersion phenomena, which can be mitigated by maximizing focusing numerical aperture (NA), employing pulse durations shorter than 10 ps and using repetition rates higher than the kHz regime [20,33].

### 3. Ultrafast Laser in Orthopedic Surgery

#### 3.1. Ablation Parameters

Early research of ultrafast laser ablation of bone tissues was predominantly focused on modification and microsurgery of teeth, ear [36] and spine, with very few publications in orthopedic surgery of the peripheral extremities (long bones of arm and leg). Despite all the advantages, the main issue that limits its clinical translation and acceptance, namely the low ablation removal rate, has remained the same even to date [35,37–39]. For instance, two studies published in 2007 discussed the use of ultrafast laser for bone ablation. Wiegner et al. conducted a comparison study of laser osteotomy on bovine bone tissues using a femtosecond (fs) Yb:glass laser (pulse duration = 330 fs;  $\lambda$  = 1040 nm; pulse repetition rate (PRR) = 1 kHz; max. average pulse energy = 130  $\mu$ J) and a conventional Er, Cr:YSGG laser system (pulse duration = 53  $\mu$ s;  $\lambda$  = 2780 nm; PRR = 20 Hz; max. average pulse energy = 300 mJ) [35]. The ablation rate of the femtosecond laser ( $\sim 4 \times 10^{-4}$  mm<sup>3</sup>/s) was found to be approximately 400-fold slower than the Erbium laser ( $\sim 0.15$  mm<sup>3</sup>/s) given a power density of  $\sim 1000$  W/cm<sup>2</sup>, but could be further optimized by increasing the PRR while maintaining the favorable cut surface morphology. The ablation thresholds were calculated to be 0.82, 0.78 and 0.54 J/cm<sup>2</sup> for spongiosa bone, compacta bone and cartilage, respectively, with an average of 72.4 laser pulses overlapped. Moreover, an ultrafast laser system consisting of a diode-pumped Yb:glass laser seed source and a Yb:KYW thin disk laser head (pulse duration = 900 fs;  $\lambda$  = 1030 nm; PRR = 45 KHz; max. average pulse energy = 100  $\mu$ J) was used by Liu et al. to achieve a maximum ablation rate of 0.15 mm<sup>3</sup>/s in porcine femora at the given power output, which was acceptable clinically for knee arthroplasty [38]. Additionally, in precision surgery such as stapedotomy, ultrafast laser has also been proven ideal by offering minimal thermal and acoustic damage [36,40].

Encouragingly, in the past decade, several studies have discovered more novel practices using ultrafast lasers and attempted to tackle the obstacles in the clinic. Notably, Subramanian et al. have developed a lightweight, miniaturized surgical ultrafast laser probe that offers clinically acceptable ablation speed in orthopedic surgery, enabling the potential of robotic integration [41]. Another group also established an optical real-time monitoring of ultrafast laser bone drilling utilizing plasma emission spectroscopy, which allowed for differentiation between bone and bone marrow [42]. The feasibility of drilling large-sized, deep holes on cortical bones has also been demonstrated [42,43]. Furthermore, the fastest ablation rate on cortical bone tissues to date is 0.99 mm<sup>3</sup>/s in the literature, which was performed on fresh ex vivo sheepshank bone under a cooling condition by Zhang et al. in 2020 [42], followed by 0.66 mm<sup>3</sup>/s on dried ex vivo defrost and dried porcine femurs under a non-cooling condition reported by Gemini et al. in 2021, using industrially available femtosecond laser sources [44], in comparison to mechanical tools that enable drilling and cutting speeds of up to 5 mm/s [45]. The upscaling of ablation rate is fundamentally constrained by the average powers combined with considerations of repetition rate optimization as well as thermal effect on the tissue [39,46]. The phenomenon arises from the fact that, at the given laser average power and wavelength, an increase in single pulse energy resulting from a decrease in PRR improves the ablation rate until the saturation point where laser energy begins to spread outside the penetration volume [47]. Gemini et al. also compared bone ablation efficiency in different wavelength regimes (IR—1030 nm, visible—515 nm, UV—343 nm), average powers (IR—6.27 W, visible—6.27 W, UV—3.9 W), PRRs (250, 500, 1000 kHz) and scanning speeds (1000, 2500, 400 mm/s) with

the conclusion that visible regime, the lowest PRR and the highest scanning speed provided the best ablation rate without thermal tissue disturbance because bone chromophores responded differently to the three wavelength regimes [44]. Moreover, the ablation rate is sometimes affected by bone debris accumulation depending on the amount generated, and thus can be further upscaled by immediate debris removal after each pulse using a cooling system [42,48]. It was demonstrated that compressed air flow and water flow could reduce bone debris by 64% and 76%, respectively; however, significant laser energy loss was observed under water cooling conditions leading to the slowest ablation rate [42]. It has also been noted that sample conditions, specifically *ex vivo* vs. *in vivo*, dried vs. fresh and storage conditions, as well as bone surface processing such as sanding, polishing or unaltered can have a significant influence on the ablation performance [49–51]; thus, it is crucial to simulate a real clinical situation for accurate and consistent assessments. Table 2 summarizes the ablation rates from ultrafast laser bone ablation studies of different bone samples using different laser parameters.

**Table 2.** Summary of recent studies on the use of ultrafast lasers for orthopedic applications.

Author/Year	Bone Type	Ablation Rate (mm <sup>3</sup> /s)	Laser System Parameters	Potential Application
Subramanian et al., 2021 [41]	Bovine rib (fresh)	$>1.7 \times 10^{-2}$	A CaF <sub>2</sub> objective; Er-doped fiber; 1552 nm, 600 fs, 303 kHz	A miniaturized surgical probe for robotic microsurgery such as spine
Gemini et al., 2021 [44]	Porcine femurs (defrost and dried)	0.66	A Tangerine industrial femtosecond laser, Amplitude Laser; 517 nm, 350 fs, 250 kHz	Clinical automated high-resolution orthopedic surgery
Ashforth et al., 2020 [49]	Bovine and ovine cortical bone (fresh)	0.90 $\mu\text{m}/\text{pulse}^*$	A Ti:Sapphire femtosecond pulsed laser; 800 nm, 140 fs, 1 kHz	Handheld or robotic high-precision orthopedic surgery procedures
Zhang et al., 2020 [42]	Sheepshank bone (fresh)	0.99	A Yb:KGW femtosecond laser; 1030 nm, 230 fs, 200 kHz	Large-size hole drilling with real-time monitoring
Aljekhedab et al., 2019 [48]	Bovine cortical bone (fresh)	$0.60 \times 10^{-3}$	A Ti:Sapphire femtosecond laser; 800 nm, 210 fs, 1 kHz	High-precision bone cutting surgery
Tulea et al., 2015 [52]	Cow femur cortical bone (fresh, dried or fixed)	0.19	A Nd:YVO <sub>4</sub> picosecond laser; 532 nm, 25 ps, 20 kHz	Bone surgery
Plötz et al., 2014 [46]	Porcine rib (fresh)	$8.7 \times 10^{-2}$	A Nd:YVO <sub>4</sub> laser; 1064 nm, 8 ps, 500 kHz	Dental surgery
Su et al., 2014 [53]	Bovine femoral condyle (fresh)	$0.80 \times 10^{-4}$	A Ti:Sapphire femtosecond laser combined with an optical parametric amplifier; 1700 nm, pulse duration N.R., 5 kHz	Microfracture surgery for articular cartilage injury in the knee

\* Reported as depth removal per pulse.

Characterization of the ablation threshold and the incubation effect likewise plays a major part in optimizing ablation performance on a particular bone type. Ablation threshold, which represents the minimal laser fluence needed to initiate material removal from a surface [39,50], can be measured by exposing the surface to ultrafast laser pulses of decreasing energy or beam radius until no material removal occurs [39,52] or using the D<sup>2</sup>-technique calculation based on the correlation between the diameters of ablated craters and different pulse energy levels [49,50,52,54–57]. Bone ablation is usually optimized when the pulse energy is sufficiently higher than the threshold to ensure pulse-to-pulse consistency, but not exceeding a limit that could induce collateral thermal damage [58]. The balance between ablation rate and fluence therefore needs to be well characterized for the bone tissue, otherwise negating the most unique advantage of minimizing thermal effects [59–61].

On the other hand, incubation effect refers to the phenomenon where a reducing ablation fluence threshold is accompanied by an increasing number of incident laser pulses in a power law relationship [62], and is typically caused by sufficient energy deposit from the few initial pulses for subsequent pulses permitting lower than single-pulse ablation threshold [41,50,57,63,64]. An incubation coefficient value of 1 indicates no incubation effect. Incubation effect is the most profound at lower pulse numbers where ablation threshold is rapidly reduced as the pulse numbers increase until a saturation point [50,65], and has been shown to modify tissue structures significantly enough, especially at higher PRR, to create beam distortion, shadowing and substantial light scattering due to debris shielding, thus leading to considerable thermal disturbance and decrease in ablation rate [44,60]. With that being said, a recent study by Ashforth et al. concluded that there was none to very little incubation effect found for two types of cortical bones (bovine and ovine) by showing the same incubation coefficient ( $1.02 \pm 0.05$ ) [49]. The possible reason, as the authors explained, could be due to the already high level of microscopic inhomogeneity of native bone tissues; the newly introduced structure defects from laser ablation were consequently negligible. For clinical translation, such behaviors are indeed beneficial in the way that the efficiency of ultrafast laser ablation can remain consistent while drilling into different bone structures. Table 3 outlines the ablation threshold for different tissue types using different laser parameters.

**Table 3.** Summary of ablation thresholds determined for different bone types. N = Number of pulses.

Author/Year	Bone Type	Ablation Threshold (J/cm <sup>2</sup> )	Pulse Duration (fs)	Wavelength (nm)
Subramanian et al., 2021 [41]	Bovine cortical bone (fresh; unaltered)	$1.38 \pm 0.18$ (N = 25.83 *; multi-pulse threshold)	600	1552
Ashforth et al., 2020 [49]	Bovine and ovine cortical bone (fresh; unaltered)	0.92 (bovine) 0.97 (ovine) (N = 1000)	140	800
Plötz et al., 2014 [46]	Porcine cortical bone (fresh; unaltered)	1.5 (N = Not Reported)	$8 \times 10^3$	1064
Cangueiro et al., 2012 [57]	Bovine cortical bone (fresh; polished)	$0.32 \pm 0.04$ (N = 100)	500	1030
Nicolodelli et al., 2012 [60]	Bovine cortical bone (fresh; polished)	0.23 (N = 1000)	70	801
Emigh et al., 2012 [50]	Porcine cortical bone (fresh; unaltered)	$1.75 \pm 0.55$ (N = 1000)	170	800
Lim et al., 2009 [63]	Bovine cortical bone (fresh; polished)	$1.22 \pm 0.29$ (strong) $0.79 \pm 0.18$ (gentle) (N = 1000)	150	775
Girard et al., 2007 [39]	Porcine cortical bone (fresh; polished)	$0.69 \pm 0.08$ (N = 1000)	200	775

\* Estimated averaged N value predicted by simulation.

### 3.2. Thermal Effect

As discussed before, ultrafast laser ablation is overall characterized by minimal thermal damage and limited heat diffusion outside of the focal volume, because the dominant mechanism, namely multiphoton absorption of light and avalanche ionization or hydrodynamic plasma expansion [66], is not thermally mediated with only little heat deposition, making it an auspicious technique in the clinic [20,67–69]. Still early studies demonstrated some carbonization, cracking and melting [53,57,60], which could be mitigated by employing cooling systems [42,70]. Nevertheless, recent studies have shown more optimized performance [34,71,72]. In particular, Ashforth et al. reported no observations of a heat-affected zone at the maximum laser fluence and pulse numbers by assessing any

forms of carbonization, discoloration and microcracking around the craters using light microscopy [49]. Canteli et al. evaluated thermal effects on fresh bovine femur using a nanosecond laser source (20 ns, 355 nm, 2–100 kHz) as compared to a picosecond laser source (12 ps, 1064 nm, 100–600 kHz), and found that the picosecond laser, although not as ideal as femtosecond lasers, resulted in significantly reduced heating compared to the nanosecond laser [71]. The study by Gemini et al. provided optimization strategies and described the observation of increasing thermal accumulation while decreasing scanning speed and increasing PRR individually in the IR and visible wavelength regimes [44]. When both the scanning speed and PRR were increased, not only thermal loads increased but expanding plasma plume was also produced, leading to reduced ablation efficiency and precision. However, the observation did not apply to the UV regime, where collagen and hemoglobin are the main absorbers. No specific behavior was detected with changing parameters; the thermal load was comparatively high enough at the lowest PRR to generate laser-induced bone calcination. In Figure 1, laser-irradiated damages such as the typical thermal-induced particle-like roughness and micro-cracks can be seen under SEM images at a higher PRR (Figure 1a), whereas native bone structures containing blood vessels and osteocytes were preserved at a lower PRR (Figure 1b,c) [44]. The interrelationship between scanning speed, PRR and wavelength choice therefore requires thorough investigation for an optimized laser ablation performance without collateral thermal damages on bone tissues. Similarly, Gill et al. studied temperature distributions of dried bovine bone irradiated also by a Tangerine laser (Amplitude, 320 fs, 1030 nm) using different PRRs [72]. It was found that carbonization occurred at high enough PRRs where thermal dissipation was exceeded by accumulation causing irreversible tissue damage, and therefore the importance of rigorous laser parameter selection was again emphasized in order to minimize thermal effects while maximizing ablation rates. Furthermore, the pattern of scanning path can also influence heat accumulation and thus reduce the ablation rate. Circular scanning motion was found to generate significant thermal damage (charring) as compared to scanning in line paths because of poor heat dissipation [42]. Additionally, with large-size and deep holes, ultrafast laser can still produce slight charring around the edge.

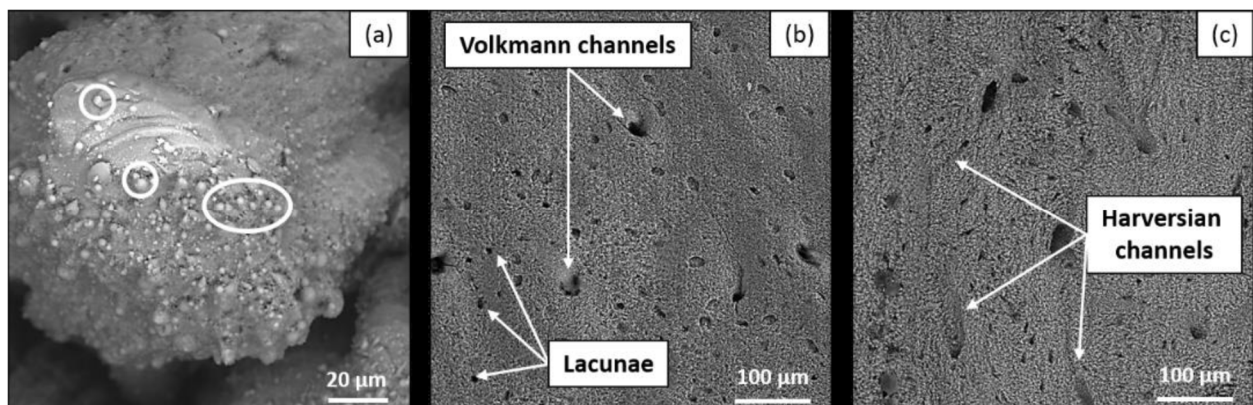


**Figure 1.** Bone tissues after ultrafast laser ablation under SEM imaging in the visible regime showing (a) laser-induced thermal damages (spherical structures indicated by the white circle) at a higher PRR (515 nm, 1000 kHz, 4000 mm/s, 6.27 W), while (b) shows native bone structures such as Volkman channels and lacunae at a lower PRR (515 nm, 250 kHz, 4000 mm/s, 6.27 W), as well as the Harversian channels shown in (c) after ablation in the IR regime (1030 nm, 250 kHz, 1000 mm/s, 6.27 W). Adapted from [44].

### 3.3. Surface Morphology

Surface morphology is usually assessed using scanning electron microscopy (SEM), confocal microscopy, X-ray computed microtomography ( $\mu$ CT) and histology to evaluate thermal effects on the tissue [42–44]. By visually examining the condition of craters or holes on bone tissue after laser ablation on the microscopic level, physical features such

as charring, roughness and micro-cracks can be identified to determine and compare the degree of laser-induced damage. As previously mentioned, a picosecond or femtosecond pulsed laser system generates little to no thermal effect during bone ablation compared to longer pulse or mechanical tools [59]. Several authors have described, under SEM or histological observations, that the bottom and side walls of the laser-ablated cavity are smooth and homogeneous with a well-defined geometry [40,48,49,71]. No significant signs of charring, melting or major debris accumulation were found [57,59,63]. Figure 2, adapted from [42], shows an image comparison of ultrafast laser ablation under different cooling conditions, namely no cooling (a, a<sub>1</sub>, a<sub>2</sub>), gas (b, b<sub>1</sub>, b<sub>2</sub>) or water (c, c<sub>1</sub>, c<sub>2</sub>) cooling, using white light imaging, SEM and histology, respectively, which demonstrated great uniformity and precise cutting with, overall, no observation of cracks, especially for cooling-assisted drillings. Some microcracks were, however, observed in the inner wall without cooling, which could potentially delay bone healing [42].

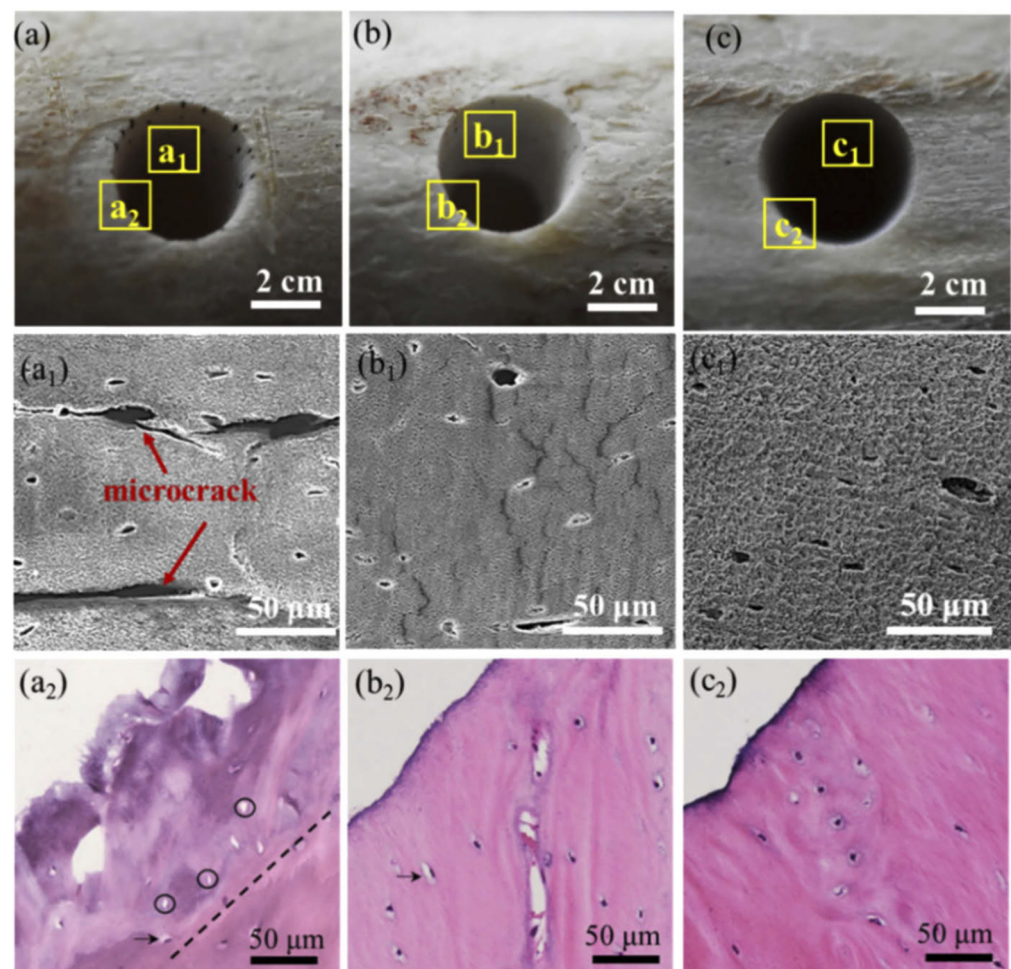


**Figure 2.** Morphology of laser-drilled bone tissues under different environmental cooling conditions. Vertical panels (a–c) correspond to without cooling, gas cooling and water cooling; horizontal panels (subscript: none, 1, 2) correspond to white light, SEM and histology images. Adapted from [42].

#### 4. Surface Modifications of Bone Implants

Another vastly studied area is surface modification of bone implants by ultrafast laser for improved osteogenesis and osteointegration. The major clinical issue present today, despite well-established implant techniques, is implant loosening owing to inadequate integration, fibrogenesis and infection [73]. Surface modification thus plays an important role to enhance cell–material interactions, and various properties can be manipulated via ultrafast laser irradiation such as surface topography, roughness and wettability [30,74].

Different nanostructures of identical materials can initiate different cellular responses and behaviors including cellular adhesion, motility, orientation and signaling pathways [75]. These factors, in short, greatly affect the success of bone implant performance, which is essentially dependent on the outcome from the complex interaction between surface characteristics and biological response. The detailed description of bone–implant interface can be found in review articles, for example, Refs [76,77]. In general, the goal of surface modification is to enhance the beneficial effects exerted on osteogenic differentiation and osteointegration of the implant [73,78]. Specifically, increasing hydrophilicity and roughness supports improved cell adhesion on an enlarged surface area as well as strong biomechanical anchorage of the implant [79,80]. Some commonly used techniques for surface roughening include grinding, polishing, sputtering and laser texturing [73]. Similar to orthopedic bone ablation, the use of ultrafast pulsed lasers (pico- or femtosecond) for surface modifications of bone implants has become attractive because of the relatively faster processing time, simpler technical requirements and minimal damage to adjacent surfaces [74,81,82]. In terms of the materials for biomedical implants, a particular attention has been paid to titanium and its alloys owing to their great biocompatibility, high resistance to temperature and corrosion as well as exceptional strength-to-weight ratio [83,84]; however, due to bio-inertness of titanium alloys, bioactivation of the material can sometimes be difficult to achieve [85]. Therefore, in this section, we briefly review recent studies on ultrafast laser surface texturing of titanium-based implants for orthopedic applications.

In recent years, femtosecond lasers have been explored extensively for surface modifications of bone implants. For example, Luo et al., investigated the ability of femtosecond lasers texturing to improve bioactivity of three types of titanium surfaces by assessing apatite deposition, a key indicator of enhanced biocompatibility and osteointegration, and found that femtosecond laser texturing could promote apatite precipitation and therefore better clinical outcomes [85]. Muck et al. examined, opposite to increasing cell adhesion, micro- and nanostructures fabricated by femtosecond laser processing to reduce cell adhesion [86]. The authors demonstrated that post-processing by electrochemical anodization following femtosecond laser treatment was able to significantly reduce cell adhesion to titanium-based flat plates and screws while promoting extracellular matrix production for osteoblasts. Figure 3 shows the SEM images of differences in osteoblast attachment to the screw and the growth on the surface between femtosecond laser processing with and without anodization. The finding suggested that the technique with its reversal could be applied to bone fixture implants that needed to be removed from the body after a period of time, i.e., less integration with the bone matrix preferred, as well as the ones that remained in the body permanently, i.e., promoted matrix growth [86]. Similar studies assessing cell adhesion and migration also concluded that femtosecond laser processing was able to improve proliferation of human mesenchymal stem cells, thus promoting osteogenesis and osteointegration [87,88]. Moreover, Liu et al. successfully prepared titanium alloy surfaces that enhanced early stage osteointegration with anti-inflammatory properties using femtosecond laser processing and sandblasting [89], again demonstrating the beneficial effects that ultrafast laser treatment could deliver. On the other hand, ultrafast laser surface processing of other biomaterials such as polyether-ether-ketone [90,91] and ceramics [92–94] has also been studied to show a comparable synergistic effect that can encourage osteointegration and osteogenesis.

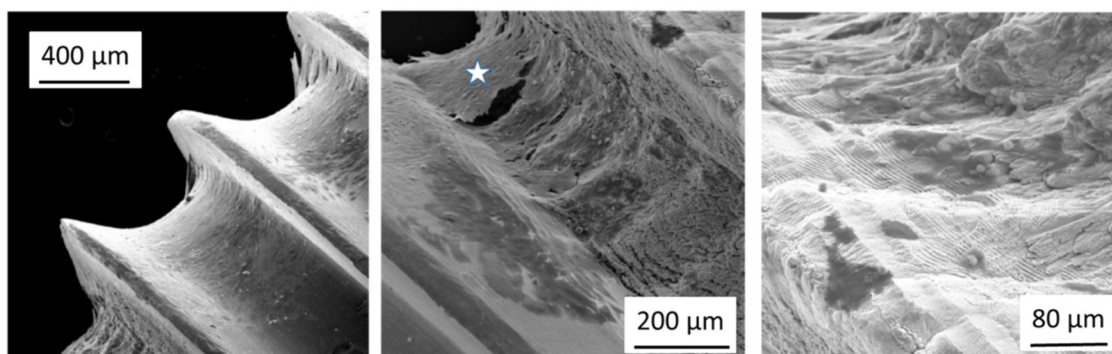


**Figure 3.** SEM image comparison of a pre-anodized titanium-based bone screw without femtosecond laser treatment (**left**) showing osteoblast growth and adhesion, and the same screw with femtosecond laser treatment (**middle**) showing cell-free areas, and details at higher magnification (**right**). Adapted from [86].

## 5. Future Direction and Conclusions

As mentioned, the intrinsic properties of ultrafast lasers provide several benefits in applications involving bone or bony structures. In comparison to conventional CW and longer wave pulse lasers that primarily depend on linear absorption of light, the nonlinear nature of ultrafast laser interaction with biological hard tissues enables unique and promising applications in the field of orthopedic surgery. As such, because of the difference present in interaction mechanisms, photodamage induced by ultrafast lasers is essentially wavelength-independent (i.e., optical properties of tissues play a minor role) with negligible thermal effects and finely controlled precision. In examining the benefits and potential use of ultrafast lasers during surgery, which can be categorized as pre-operative, intraoperative and post-operative advantages, there will be a focus on pre-operative and intraoperative strategies since post-operative utilizations, namely wound healing and tissue bonding, have been extensively reviewed elsewhere [20,95,96]. In addition to this, we will speak to the technical challenges encountered so far, which preclude ultrafast lasers from widespread clinical adoption. Finally, future research directions that are of potential interest clinically will be discussed.

### 5.1. Applications

In terms of pre-surgical applications of ultrafast lasers in orthopedic surgery, the main benefit would be the preparation of implants or materials for integration within bone. For instance, Liu et al. [89] and Muck et al. [86] have demonstrated how ultrafast laser machining increases osteointegration and biocompatibility. Taking these into consideration, it could be envisioned that implants in total hip arthroplasty and total knee arthroplasty would be patterned to increase osteointegration of the implants without necessitating the use of bone cement or other anchors, such as intramedullary nailing or percutaneous screws. Although an uncommon complication, early failure of implants occurs in both knee and hip arthroplasty, either due to failure of bone cement to anchor the implant causing loosening and loss of stability, or contact with surrounding bone when using a cementless implant, leading to a similar outcome [97,98]. Revision surgeries in these cases provide worse outcomes compared to the primary surgery, with higher rates of infection, worse overall prognosis and delayed healing, especially in patients with preexisting comorbidities and poor overall health [99]. Thus, ultrafast laser machining of the implant surface could mitigate failure rates and improved overall outcomes. However, it should be noted that during many of these surgeries, it is not known a priori what implant or which size the surgeon will choose as it is dependent on the size of bored hole in the femur/tibia or the size of the acetabulum.

In these cases of furthering the osteointegrative potential of hip and knee arthroplasty implants, there are two approaches in which femtosecond laser surface modification could

be used. In the first use case, all implants have surface preparation performed with ultrafast lasers at the time of manufacturing prior to shipment to various orthopedic centers. If the cost or time of surface preparation is not a feasible option, a second approach would be for the surgeon to identify high-risk patients where implant failure may occur and prepare these devices accordingly. Furthermore, many medical device manufacturers have explored the use of 3D printing of custom implants based on preoperative imaging where ultrafast laser surface modification in combination with custom 3D-printed joint implants could provide an overall increase in mobility and function following surgery for these high-risk patients. Thus, ultrafast laser surface preparation in conjunction with custom implant manufacturing, where an increase in osteointegration contributes to the overall well-being of the patient, provides a greater impetus for both custom implant manufacturing as well as increases in overall outcome. Future work would examine the use of ultrafast laser patterning on materials outside of the traditional knee arthroplasty and hip arthroplasty components, as 3D-printed joint replacement can use highly porous materials that are prone to heat damage and warping [100]. Additionally, recent studies have demonstrated higher migration rates (implant slides 'upwards' from where it was set) for cementless 3D-printed joint 'stems' in knee and hip arthroplasty [101]. This migration of the implant away from where it is set is an indicator of impending aseptic loosening, which normally necessitates a revision procedure, whereby surface preparation and increased implant anchoring provides a tangible benefit to both patients and operators, since, as discussed, revision surgery is a costly and detrimental procedure.

Secondly, to preparation of implants or materials, a large area of research for the use of ultrafast lasers is cutting of hard surfaces, specifically dentine, enamel and bone. Specifically, it was noted in early studies on dentine ablation that ultrafast laser cutting provided limited thermal deposition with increased cellular survival surrounding the ablation area. This contrasts with the use of electrocautery (EC) or burrs/saws/trephines, where frictional forces during cutting cause a large amount of heat deposition to the surrounding tissues outside of bone, leading to potential cell damage with complications such as nerve damage, bleeding from injured vessels and delayed healing of the cutting surface. In these cases, the non-thermal nature of ultrafast lasers provides an opportunity for use in procedures that are performed adjacent to sensitive tissues. These procedures need a safety margin to protect sensitive tissues; for example, transsphenoidal resection or laminectomy, involving cutting and removal of bone close to the central nervous system, specifically the pituitary gland and CSF/dura in transsphenoidal resection and the CSF/dura and the spine in laminectomy, or close to vessels, such as in brain surgery in the posterior cranial fossa, where venous sinuses and arteries are located. Utilizing ultrafast laser cutting in lieu of mechanical drills in transsphenoidal resection or laminectomy, therefore, would be of benefit in reducing or eliminating thermal deposition in surrounding tissues compared to a high-speed mechanical burr or trephine alone, providing a greater safety margin in the procedures where critical tissue is nearby. Furthermore, this could be generalized to many approaches in the skull, whereby CNS/dura is invariably adjacent; for example, thermal injury has been demonstrated in retrosigmoid intradural suprameatal approach (RISA), with cutting through bone leading to injury of the petrosal sinuses and nerve with possible cerebellar swelling and infarction following [102]. Thus, with limited heat generation, ultrafast laser ablation could be adopted for procedures whereby limiting adjacent thermal damage should reduce any unintended consequences from already complex surgeries to begin with.

### 5.2. Technical Challenges

Despite the readily apparent advantages with ultrafast lasers, there has been limited adoption to date, even in applications where the benefits are obvious. The most pressing challenge surrounding the use of ultrafast laser is the ablation rate compared to conventional laser ablation systems (and their associated drawbacks including carbonization) and mechanical drilling. It has been described in multiple studies that a femtosecond

laser system provides an ablation rate of approximately 1  $\mu\text{m}/\text{pulse}$  in hard tissue such as bone at a repetition rate of 10 Hz [36,103]. This is compared to up to 30  $\mu\text{m}/\text{pulse}$  for Er:YAG laser systems at a pulse rate of 4 Hz. At this repetition rate, the ablation rate would be 10  $\mu\text{m}/\text{s}$ , compared to 120  $\mu\text{m}/\text{s}$  for conventional laser systems. This can be further compared to mechanical drilling rates of 4–5 mm/s with larger burrs/drill bits that can achieve the ablation volume in a much shorter time. Research is ongoing into higher repetition rate femtosecond laser systems (upwards of 40 KHz) that would mitigate some of the differences through matching the ablation rate; however, the volume ablated per time is still inherently mismatched due to the size of mechanical drilling devices compared to the spot size of ultrafast laser devices [44]. Due to the time constraints of many public operating rooms and the number of patients requiring procedures such as hip and knee arthroplasty, the ablation rate would be required to come close to matching the shaving/feed rate of high-speed mechanical drills for clinical translation.

A second technical challenge for ultrafast laser systems is the adoption of these systems into endoscopic devices for minimally invasive surgery. These approaches are becoming more prevalent in all surgeries including orthopedic due to the potential for reduced tissue trauma and quicker recovery. In these approaches, such as transsphenoidal access or laminectomy, the limitation of ultrafast laser fibers in terms of attenuation and dispersion characteristics have precluded the adoption into endoscopes that are currently in use. Although fibers have been developed for implementation into an endoscope, the cutting power, modal quality, dispersion and attenuation are dependent on the bending radius, compromising cutting efficiency or ablation rates in these applications altogether. Ongoing research of fibers for integration into endoscopes, which are flexible enough to generate continuous power input, provides the basis to suggest that this problem will be overcome and adoption would be able to proceed [104–106].

### 5.3. Future Directions

In the scenarios envisioned where ultrafast lasers would potentially be of benefit, there are number of future directions that should be addressed and examined. Firstly, a method to stop laser ablation as soon as the bone is cut through to prevent a similar laser-induced ‘plunge’ into tissue such as dura or nervous tissue would need to be developed, similar to the mechanical chuck that has been integrated into cranial perforators [107]. Plunging into inferior tissues such as the dura and/or brain would be of greater detriment compared to any gains made from reduced thermal deposition and reduced thermal damage from either direct brain damage or CSF leakage. A high degree of pre-planning using CT or MRI to determine bone thickness as well as depth control during the procedure would need to be achieved to prevent overcutting at any given volume currently being ablated. This degree of intraoperative control of cutting/ablation would, at a minimum, require a guidance platform demonstrated in procedures such as pedicle screw placement whereby IR based navigation is used to track the screw in real time with combined CT guidance [108], and the laser tip/front could be tracked in real time. A second approach would be to combine the ultrafast laser cutting tool with an optical approach such as diffuse reflectance spectroscopy (DRS) where optical properties of incoming tissue can be measured in real time. In combining DRS with ultrafast laser cutting/ablation, the relatively slower speed of laser-based ablation would allow for DRS measurements in combination with real-time optical property measurements, enabling in-line tissue differentiation. Nonetheless, a system of external tracking, such as IR navigation, or with fiber measurements of optical properties, such as DRS, would need to be implemented to prevent overcutting of tissue, leading to dural laceration or nerve/vessel injury that would provide no appreciable benefit to conventional surgical techniques.

Secondly, we propose that in the transition of the use of ultrafast lasers into bone surgery, integration either within a robotic or navigation platform will be necessary to allow for higher success chance in the proposed applications [109]. As mentioned previously, cutting depth is an important parameter in the procedures such as laminectomy

or transsphenoidal placement. Surgeons currently use a combination of auditory cues and haptic feedback when assessing depth while drilling, and would not be able to use a laser-based cutting/ablation approach. We propose that a robotic platform could be developed, including either a navigation device or optical 'guidance' system such as DRS. The addition of these platforms can overcome the loss of haptic feedback and auditory cues normally used by surgeons while maintaining the safety of the procedure. This can be expanded to include semi-autonomous or AI-driven robotic platforms where surgeons design cutting paths in conjunction with a robotic laser-based system that could perform cutting procedures, such as removal of the sphenoid bone or lamina with minimal surgeon oversight. This type of platform is appealing as it would lead to a reduction in exposure to X-rays to both patient and operators, commonly encountered in many orthopedic procedures and secondly, increase overall outcomes due to increased osteointegration and reduced thermal deposition.

Finally, laser systems and fibers need to be developed that can provide both high ablation rates and flexibility that would allow for integration into currently existing minimally invasive surgical devices. In terms of ablation rates, the rate would need to at least approximate the ablation rate of mechanical drills (4–5 mm/s) as well as approximating the ablation volume. For example, in orthopedic surgery the drill bit size would be 6–8 mm with the aforementioned ablation rate in procedures such as hip and knee arthroplasty. It could be argued that with the added benefits of limited thermal deposition and improved wound healing, some leeway could be given to the ablation rate of bone; however, it needs to be fast enough to not unduly delay these procedures. With this in mind, ultrafast laser systems would be more beneficial in endoscopic-based ablation procedures where the ablation rate is not the limiting factor with the burrs commonly used being much smaller (0.5–1.0 mm), and thus the gap between ablation volume not as large. In these procedures, the benefits of ultrafast laser ablation combined with the more closely matched laser spot size and burr size would allow for an easier transition without unduly delaying any procedures. In this case, fiber development would need to allow for shaper bending radii without an impact on laser performance.

#### 5.4. Conclusions

In examining the osteointegrative potential and hard tissue ablation, the use of ultrafast lasers in a number of surgical procedures such as total/hip knee arthroplasty, laminectomy and transsphenoidal resection could lead to meaningful benefits to both patients and operators; specifically, surface treatment of custom 3D-printed implants for patients, where ultrafast laser modification could address one of the limitations of increased implant loosening without the use of cement and lead to further adoption. In addition, reduced thermal damage to surrounding tissues with laser cutting/ablation in areas adjacent to critical structures, such as in transsphenoidal resection, highlights one of the benefits ultrafast lasers can provide. Overall, with further research, specifically in flexible fiber technology without loss of ablation potential, ultrafast lasers can provide a meaningful change in outcomes and workflows in the surgical procedures highlighted.

**Author Contributions:** Conceptualization, C.L.L. and C.J.F.; Investigation, C.L.L. and C.J.F.; Writing—Original Draft Preparation, C.L.L.; Writing—Review & Editing, C.L.L., C.J.F., R.B. and S.A.-E.; Visualization, C.L.L.; Supervision, S.A.-E.; Project Administration, R.B. and S.A.-E.; Funding Acquisition, S.A.-E. All authors have read and agreed to the published version of the manuscript.

**Funding:** This work was supported by Science Foundation Ireland (SFI), Grant No. SFI/15/RP/2828.

**Institutional Review Board Statement:** Not applicable.

**Informed Consent Statement:** Not applicable.

**Data Availability Statement:** No new data were created or analyzed in this study. Data sharing is not applicable to this article.

**Conflicts of Interest:** The authors declare no conflict of interest.

## References

1. Gunaratne, G.D.R.; Khan, R.; Fick, D.; Robertson, B.; Dahotre, N.; Ironside, C. A review of the physiological and histological effects of laser osteotomy. *J. Med. Eng. Technol.* **2017**, *41*, 1–12. [[CrossRef](#)] [[PubMed](#)]
2. Sotsuka, Y.; Nishimoto, S.; Tsumano, T.; Kawai, K.; Ishise, H.; Kakibuchi, M.; Shimokita, R.; Yamauchi, T.; Okihara, S.-I. The dawn of computer-assisted robotic osteotomy with ytterbium-doped fiber laser. *Lasers Med. Sci.* **2014**, *29*, 1125–1129. [[CrossRef](#)] [[PubMed](#)]
3. Stübinger, S.; Ghanaati, S.; Saldamli, B.; Kirkpatrick, C.J.; Sader, R. Er:YAG Laser Osteotomy: Preliminary Clinical and Histological Results of a New Technique for Contact-Free Bone Surgery. *Eur. Surg. Res.* **2009**, *42*, 150–156. [[CrossRef](#)] [[PubMed](#)]
4. Asnaashari, M.; Zadsirjan, S. Application of Laser in Oral Surgery. *J. Lasers Med. Sci.* **2014**, *5*, 97–107. [[CrossRef](#)] [[PubMed](#)]
5. Parker, S.; Cronshaw, M.; Anagnostaki, E.; Mylona, V.; Lynch, E.; Grootveld, M. Current Concepts of Laser–Oral Tissue Interaction. *Dent. J.* **2020**, *8*, 61. [[CrossRef](#)] [[PubMed](#)]
6. Davoudi, A.; Amrolahi, M.; Khaki, H. Effects of laser therapy on patients who underwent rapid maxillary expansion; a systematic review. *Lasers Med. Sci.* **2018**, *33*, 1387–1395. [[CrossRef](#)]
7. Radcliff, K.; Vaccaro, A.R.; Hilibrand, A.; Schroeder, G.D. Lasers in Spine Surgery. *J. Am. Acad. Orthop. Surg.* **2019**, *27*, 621–632. [[CrossRef](#)]
8. Ahn, Y.; Lee, U. Use of lasers in minimally invasive spine surgery. *Expert Rev. Med. Devices* **2018**, *15*, 423–433. [[CrossRef](#)]
9. Kong, X.; Wakida, N.M.; Yokomori, K. Application of Laser Microirradiation in the Investigations of Cellular Responses to DNA Damage. *Front. Phys.* **2021**, *8*, 628. [[CrossRef](#)]
10. Miller, P.R.; Aggarwal, R.; Doraiswamy, A.; Lin, Y.J.; Lee, Y.-S.; Narayan, R.J. Laser micromachining for biomedical applications. *JOM* **2009**, *61*, 35–40. [[CrossRef](#)]
11. Krueger, A. Ultrafast lasers in biophotonics. In *Multiphoton Microscopy and Fluorescence Lifetime Imaging*; Walter de Gruyter GmbH & Co KG: Berlin, Germany, 2018; ISBN 9783110429985.
12. Tzanakakis, E.-G.C.; Skoulas, E.; Pepelassi, E.; Koidis, P.; Tzoutzas, I.G. The Use of Lasers in Dental Materials: A Review. *Materials* **2021**, *14*, 3370. [[CrossRef](#)] [[PubMed](#)]
13. Petrov, T.; Pecheva, E.; Walmsley, A.D.; Dimov, S. Femtosecond laser ablation of dentin and enamel for fast and more precise dental cavity preparation. *Mater. Sci. Eng. C* **2018**, *90*, 433–438. [[CrossRef](#)] [[PubMed](#)]
14. Luengo, M.C.L.; Portillo, M.; Sánchez, J.M.; Peix, M.; Moreno, P.; García, A.; Montero, J.; Albaladejo, A. Evaluation of micromorphological changes in tooth enamel after mechanical and ultrafast laser preparation of surface cavities. *Lasers Med. Sci.* **2013**, *28*, 267–273. [[CrossRef](#)] [[PubMed](#)]
15. Chen, H.; Li, H.; Sun, Y.C.; Wang, Y.; Lü, P.F. Femtosecond laser for cavity preparation in enamel and dentin: Ablation efficiency related factors. *Sci. Rep.* **2016**, *6*, 20950. [[CrossRef](#)]
16. Pantawane, M.V.; Dahotre, N.B. Challenges and Advances in Osteotomy. *Ann. Bone Jt. Surg.* **2019**, *2*, 1–4. [[CrossRef](#)]
17. Troedhan, A.; Mahmoud, Z.T.; Wainwright, M.M.; Khamis, M. Cutting bone with drills, burs, lasers and piezotomes: A comprehensive systematic review and recommendations for the clinician. *Int. J. Oral Craniofacial Sci.* **2017**, *3*, 20–33. [[CrossRef](#)]
18. Azadgoli, B.; Baker, R.Y. Laser applications in surgery. *Ann. Transl. Med.* **2016**, *4*, 452. [[CrossRef](#)]
19. Khalkhal, E.; Rezaei-Tavirani, M.; Zali, M.R.; Akbari, Z. The Evaluation of Laser Application in Surgery: A Review Article. *J. Lasers Med. Sci.* **2019**, *10*, S104–S111. [[CrossRef](#)]
20. Hoy, C.L.; Ferhanoglu, O.; Yildirim, M.; Kim, K.H.; Karajanagi, S.S.; Chan, K.M.C.; Kobler, J.B.; Zeitels, S.M.; Ben-Yakar, A. Clinical Ultrafast Laser Surgery: Recent Advances and Future Directions. *IEEE J. Sel. Top. Quantum Electron.* **2014**, *20*, 710081. [[CrossRef](#)]
21. Bernal, L.M.B.; Canbaz, F.; Droneau, A.; Friederich, N.F.; Cattin, P.C.; Zam, A. Optimizing deep bone ablation by means of a microsecond Er:YAG laser and a novel water microjet irrigation system. *Biomed. Opt. Express* **2020**, *11*, 7253–7272. [[CrossRef](#)]
22. Nuss, R.C.; Fabian, R.L.; Sarkar, R.; Puliafito, C.A. Infrared laser bone ablation. *Lasers Surg. Med.* **1988**, *8*, 381–391. [[CrossRef](#)] [[PubMed](#)]
23. Lee, C.L.; Roberts, C.; Litsky, A.S. Laser Ablation of Dyed Acrylic Bone Cement. *Lasers Surg. Med.* **1997**, *20*, 280–289. [[CrossRef](#)]
24. Ivanenko, M.; Werner, M.; Afilal, S.; Klasing, M.; Hering, P. Ablation of hard bone tissue with pulsed CO<sub>2</sub> lasers. *Med. Laser Appl.* **2005**, *20*, 13–23. [[CrossRef](#)]
25. Carr, C.W.; Radousky, H.B.; Demos, S.G. Wavelength Dependence of Laser-Induced Damage: Determining the Damage Initiation Mechanisms. *Phys. Rev. Lett.* **2003**, *91*, 127402. [[CrossRef](#)] [[PubMed](#)]
26. Kohli, V.; Elezzabi, A.Y.; Acker, J.P. Cell nanosurgery using ultrashort (femtosecond) laser pulses: Applications to membrane surgery and cell isolation. *Lasers Surg. Med.* **2005**, *37*, 227–230. [[CrossRef](#)] [[PubMed](#)]
27. Ii, J.E.M.; Kim, B.-M. Medical applications of ultrashort-pulse lasers. In *Commercial and Biomedical Applications of Ultrafast Lasers*; SPIE: Bellingham, WA, USA, 1999; pp. 42–50. [[CrossRef](#)]
28. Vogel, A.; Venugopalan, V. Mechanisms of Pulsed Laser Ablation of Biological Tissues. *Chem. Rev.* **2003**, *103*, 577–644. [[CrossRef](#)]
29. Sheetz, K.E.; Squier, J. Ultrafast optics: Imaging and manipulating biological systems. *J. Appl. Phys.* **2009**, *105*, 051101. [[CrossRef](#)]
30. Canguero, L.T.; Le Quang, T.; Vilar, R. Laser surface modification of biological hard tissues. In *Laser Surface Modification of Biomaterials: Techniques and Applications*; Elsevier Ltd.: Amsterdam, The Netherlands, 2016; pp. 221–251, ISBN 9780081009420.
31. Isobe, K.; Watanabe, W.; Itoh, K. Ultrafast Laser Surgery. In *Functional Imaging by Controlled Nonlinear Optical Phenomena*; John Wiley & Sons: Hoboken, NJ, USA, 2013; pp. 660–688, ISBN 9781626239777.

32. Jeong, D.C.; Tsai, P.S.; Kleinfeld, D. Prospect for feedback guided surgery with ultra-short pulsed laser light. *Curr. Opin. Neurobiol.* **2012**, *22*, 24–33. [[CrossRef](#)]
33. Vogel, A.; Noack, J.; Hüttman, G.; Paltauf, G. Mechanisms of femtosecond laser nanosurgery of cells and tissues. *Appl. Phys. B* **2005**, *81*, 1015–1047. [[CrossRef](#)]
34. Domke, M.; Wick, S.; Laible, M.; Rapp, S.; Huber, H.P.; Sroka, R. Ultrafast dynamics of hard tissue ablation using femtosecond-lasers. *J. Biophotonics* **2018**, *11*, e201700373. [[CrossRef](#)]
35. Wieger, V.; Zoppel, S.; Wintner, E. Ultrashort pulse laser osteotomy. *Laser Phys.* **2007**, *17*, 438–442. [[CrossRef](#)]
36. Armstrong, W.B.; Neev, J.A.; Da Silva, L.B.; Rubenchik, A.M.; Stuart, B.C. Ultrashort pulse laser ossicular ablation and stapedotomy in cadaveric bone. *Lasers Surg. Med.* **2002**, *30*, 216–220. [[CrossRef](#)] [[PubMed](#)]
37. Strassl, M.; Wieger, V.; Brodoceanu, D.; Beer, F.; Moritz, A.; Wintner, E. Ultra-Short Pulse Laser Ablation of Biological Hard Tissue and Biocompatibles. *J. Laser Micro/Nanoeng.* **2008**, *3*, 30–40. [[CrossRef](#)]
38. Liu, Y.; Niemz, M. Ablation of femoral bone with femtosecond laser pulses—A feasibility study. *Lasers Med. Sci.* **2007**, *22*, 171–174. [[CrossRef](#)] [[PubMed](#)]
39. Girard, B.; Yu, D.; Armstrong, M.R.; Wilson, B.C.; Clokie, C.M.L.; Miller, R.J.D. Effects of femtosecond laser irradiation on osseous tissues. *Lasers Surg. Med.* **2007**, *39*, 273–285. [[CrossRef](#)] [[PubMed](#)]
40. McCaughey, R.G.; Sun, H.; Rothholtz, V.S.; Juhasz, T.; Wong, B.J.-F. Femtosecond laser ablation of the stapes. *J. Biomed. Opt.* **2009**, *14*, 024040. [[CrossRef](#)] [[PubMed](#)]
41. Subramanian, K.; Andrus, L.; Pawlowski, M.; Wang, Y.; Tkaczyk, T.; Ben-Yakar, A. Ultrafast laser surgery probe with a calciumfluoride miniaturized objective for bone ablation. *Biomed. Opt. Express* **2021**, *12*, 4779. [[CrossRef](#)]
42. Zhang, J.; Guan, K.; Zhang, Z.; Guan, Y. In vitro evaluation of ultrafast laser drilling large-size holes on sheepshank bone. *Opt. Express* **2020**, *28*, 25528. [[CrossRef](#)]
43. An, R.; Khadar, G.W.; Wilk, E.I.; Emigh, B.; Haugen, H.K.; Wohl, G.R.; Dunlop, B.; Anvari, M.; Hayward, J.E.; Fang, Q. Ultrafast laser ablation and machining large-size structures on porcine bone. *J. Biomed. Opt.* **2013**, *18*, 070504. [[CrossRef](#)]
44. Gemini, L.; Al-Bourgol, S.; Machinet, G.; Bakkali, A.; Faucon, M.; Kling, R. Ablation of Bone Tissue by Femtosecond Laser: A Path to High-Resolution Bone Surgery. *Materials* **2021**, *14*, 2429. [[CrossRef](#)]
45. Fisher, C.; Harty, J.; Yee, A.; Li, C.L.; Komolibus, K.; Grygoryev, K.; Lu, H.; Burke, R.; Wilson, B.C.; Andersson-Engels, S. Perspective on the integration of optical sensing into orthopedic surgical devices. *J. Biomed. Opt.* **2022**, *27*, 010601. [[CrossRef](#)] [[PubMed](#)]
46. Plötz, C.; Schelle, F.; Bourauel, C.; Frentzen, M.; Meister, J. Ablation of porcine bone tissue with an ultrashort pulsed laser (USPL) system. *Lasers Med. Sci.* **2014**, *30*, 977–983. [[CrossRef](#)] [[PubMed](#)]
47. Kramer, T.; Remund, S.; Jäggi, B.; Schmid, M.; Neuenschwander, B. Ablation dynamics—From absorption to heat accumulation/ultra-fast laser matter interaction. *Adv. Opt. Technol.* **2018**, *7*, 129–144. [[CrossRef](#)]
48. Aljekhedab, F.; Zhang, W.; Haugen, H.K.; Wohl, G.R.; El-Desouki, M.M.; Fang, Q. Influence of environmental conditions in bovine bone ablation by ultrafast laser. *J. Biophotonics* **2019**, *12*, e201800293. [[CrossRef](#)] [[PubMed](#)]
49. Ashforth, S.A.; Oosterbeek, R.N.; Bodley, O.L.C.; Mohr, C.; Aguegaray, C.; Simpson, M.C. Femtosecond lasers for high-precision orthopedic surgery. *Lasers Med. Sci.* **2020**, *35*, 1263–1270. [[CrossRef](#)] [[PubMed](#)]
50. Emigh, B.; An, R.; Hsu, E.M.; Crawford, T.H.R.; Haugen, H.K.; Wohl, G.R.; Hayward, J.E.; Fang, Q. Porcine cortical bone ablation by ultrashort pulsed laser irradiation. *J. Biomed. Opt.* **2012**, *17*, 0280011–0280016. [[CrossRef](#)]
51. Kim, B.; Feit, M.D.; Rubenchik, A.M.; Joslin, E.J.; Eichler, J.; Stoller, P.C.; Da Silva, L.B. Effects of high repetition rate and beam size on hard tissue damage due to subpicosecond laser pulses. *Appl. Phys. Lett.* **2000**, *76*, 4001–4003. [[CrossRef](#)]
52. Tulea, C.; Caron, J.; Gehlich, N.; Lenenbach, A.; Noll, R.; Loosen, P. Laser cutting of bone tissue under bulk water with a pulsed ps-laser at 532 nm. *J. Biomed. Opt.* **2015**, *20*, 105004. [[CrossRef](#)]
53. Su, E.; Sun, H.; Juhasz, T.; Wong, B.J.F. Preclinical investigations of articular cartilage ablation with femtosecond and pulsed infrared lasers as an alternative to microfracture surgery. *J. Biomed. Opt.* **2014**, *19*, 098001. [[CrossRef](#)]
54. Mannion, P.T.; Magee, J.; Coyne, E.; O'Connor, G.M.; Glynn, T.J. The effect of damage accumulation behaviour on ablation thresholds and damage morphology in ultrafast laser micro-machining of common metals in air. *Appl. Surf. Sci.* **2004**, *233*, 275–287. [[CrossRef](#)]
55. Ben-Yakar, A.; Byer, R.L. Femtosecond laser ablation properties of borosilicate glass. *J. Appl. Phys.* **2004**, *96*, 5316–5323. [[CrossRef](#)]
56. Liu, J.M. Simple technique for measurements of pulsed Gaussian-beam spot sizes. *Opt. Lett.* **1982**, *7*, 196–198. [[CrossRef](#)] [[PubMed](#)]
57. Canguero, L.T.; Vilar, R.; do Rego, A.M.B.; Muralha, V.S.F. Femtosecond laser ablation of bovine cortical bone. *J. Biomed. Opt.* **2012**, *17*, 125005. [[CrossRef](#)] [[PubMed](#)]
58. Mortensen, L.J.; Alt, C.; Turcotte, R.; Masek, M.; Liu, T.-M.; Côté, D.C.; Xu, C.; Intini, G.; Lin, C.P. Femtosecond laser bone ablation with a high repetition rate fiber laser source. *Biomed. Opt. Express* **2015**, *6*, 32–42. [[CrossRef](#)]
59. Lo, D.D.; Mackanos, M.A.; Chung, M.T.; Hyun, J.S.; Montoro, D.T.; Grova, M.; Liu, C.; Wang, J.; Palanker, D.; Connolly, A.J.; et al. Femtosecond plasma mediated laser ablation has advantages over mechanical osteotomy of cranial bone. *Lasers Surg. Med.* **2012**, *44*, 805–814. [[CrossRef](#)]
60. Nicolodelli, G.; Lizarelli, R.D.F.Z.; Bagnato, V.S. Influence of effective number of pulses on the morphological structure of teeth and bovine femur after femtosecond laser ablation. *J. Biomed. Opt.* **2012**, *17*, 048001. [[CrossRef](#)]

61. Nguyen, J.; Ferdman, J.; Zhao, M.; Huland, D.; Saqqa, S.; Ma, J.; Nishimura, N.; Schwartz, T.H.; Schaffer, C.B. Sub-surface, micrometer-scale incisions produced in rodent cortex using tightly-focused femtosecond laser pulses. *Lasers Surg. Med.* **2011**, *43*, 382–391. [[CrossRef](#)]
62. Jee, Y.; Becker, M.F.; Walser, R.M. Laser-induced damage on single-crystal metal surfaces. *J. Opt. Soc. Am. B* **1988**, *5*, 648–659. [[CrossRef](#)]
63. Lim, Y.C.; Altman, K.J.; Farson, D.F.; Flores, K.M. Micropillar fabrication on bovine cortical bone by direct-write femtosecond laser ablation. *J. Biomed. Opt.* **2009**, *14*, 064021. [[CrossRef](#)]
64. Marjoribanks, R.S.; Dille, C.; Schoenly, J.E.; McKinney, L.; Mordovanakis, A.; Kaifosh, P.; Forrester, P.; Qian, Z.; Covarrubias, A.; Feng, Y.; et al. Ablation and thermal effects in treatment of hard and soft materials and biotissues using ultrafast-laser pulse-train bursts. *Photon. Lasers Med.* **2012**, *1*, 155–169. [[CrossRef](#)]
65. Rosenfeld, A.; Lorenz, M.; Stoian, R.; Ashkenasi, D. Ultrashort-laser-pulse damage threshold of transparent materials and the role of incubation. *Appl. Phys. A* **1999**, *69*, S373–S376. [[CrossRef](#)]
66. Stuart, B.C.; Feit, M.D.; Rubenchik, A.M.; Shore, B.W.; Perry, M.D. Laser-Induced Damage in Dielectrics with Nanosecond to Subpicosecond Pulses. *Phys. Rev. Lett.* **1995**, *74*, 2248–2251. [[CrossRef](#)] [[PubMed](#)]
67. Lee, Y.M.; Tu, R.Y.; Chiang, A.C.; Huang, Y.C. Average-power mediated ultrafast laser osteotomy using a mode-locked Nd:YVO[sub 4] laser oscillator. *J. Biomed. Opt.* **2007**, *12*, 060505. [[CrossRef](#)] [[PubMed](#)]
68. Daskalova, A.; Bashir, S.; Husinsky, W. Morphology of ablation craters generated by ultra-short laser pulses in dentin surfaces: AFM and ESEM evaluation. *Appl. Surf. Sci.* **2010**, *257*, 1119–1124. [[CrossRef](#)]
69. Kim, B.; Feit, M.D.; Rubenchik, A.M.; Joslin, E.J.; Celliers, P.; Eichler, J.; Da Silva, L.B. Influence of pulse duration on ultrashort laser pulse ablation of biological tissues. *J. Biomed. Opt.* **2001**, *6*, 332–338. [[CrossRef](#)]
70. Friedrich, R.E.; Quade, M.; Jowett, N.; Kroetz, P.; Amling, M.; Kohlrusch, F.K.; Zustin, J.; Gosau, M.; Schlüter, H.; Miller, R.J.D. Ablation Precision and Thermal Effects of a Picosecond Infrared Laser (PIRL) on Roots of Human Teeth: A Pilot Study Ex Vivo. *In Vivo* **2020**, *34*, 2325–2336. [[CrossRef](#)]
71. Canteli, D.; Muñoz-García, C.; Morales, M.; Márquez, A.; Lauzurica, S.; Arregui, J.; Lazkoz, A.; Molpeceres, C. Thermal Effects in the Ablation of Bovine Cortical Bone with Pulsed Laser Sources. *Materials* **2019**, *12*, 2916. [[CrossRef](#)]
72. Gill, R.K.; Smith, Z.J.; Lee, C.; Wachsmann-Hogiu, S. The effects of laser repetition rate on femtosecond laser ablation of dry bone: A thermal and LIBS study. *J. Biophotonics* **2016**, *9*, 171–180. [[CrossRef](#)]
73. Stich, T.; Alagboso, F.; Křenek, T.; Kovářik, T.; Alt, V.; Docheva, D. Implant-bone-interface: Reviewing the impact of titanium surface modifications on osteogenic processes in vitro and in vivo. *Bioeng. Transl. Med.* **2022**, *7*, e10239. [[CrossRef](#)]
74. Cunha, W.; Carvalho, O.; Henriques, B.; Silva, F.S.; Özcan, M.; Souza, J.C.M. Surface modification of zirconia dental implants by laser texturing. *Lasers Med. Sci.* **2022**, *37*, 77–93. [[CrossRef](#)]
75. Jones, J.R. Observing cell response to biomaterials. *Mater. Today* **2006**, *9*, 34–43. [[CrossRef](#)]
76. Shah, F.A.; Thomsen, P.; Palmquist, A. Osseointegration and current interpretations of the bone-implant interface. *Acta Biomater.* **2019**, *84*, 1–15. [[CrossRef](#)] [[PubMed](#)]
77. Faucheux, N.; Beauvais, S.; Drevelle, O.; Jann, J.; Lauzon, M.-A.; Foruzanmehr, M.; Grenier, G.; Roux, S. Interactions between bone cells and biomaterials: An update. *Front. Biosci.* **2016**, *8*, 227–263. [[CrossRef](#)] [[PubMed](#)]
78. Calciolari, E.; Hamlet, S.; Ivanovski, S.; Donos, N. Pro-osteogenic properties of hydrophilic and hydrophobic titanium surfaces: Crosstalk between signalling pathways in vivo models. *J. Periodontal Res.* **2018**, *53*, 598–609. [[CrossRef](#)] [[PubMed](#)]
79. Wang, W.; Caetano, G.; Ambler, W.S.; Blaker, J.J.; Frade, M.A.; Mandal, P.; Diver, C.; Bártolo, P. Enhancing the Hydrophilicity and Cell Attachment of 3D Printed PCL/Graphene Scaffolds for Bone Tissue Engineering. *Materials* **2016**, *9*, 992. [[CrossRef](#)]
80. Wei, S.; Deng, Y.; Liu, X.; Xu, A.; Wang, L.; Luo, Z.; Zheng, Y.; Deng, F.; Tang, Z.; Wei, J. Effect of surface roughness on osteogenesis in vitro and osseointegration in vivo of carbon fiber-reinforced polyetheretherketone–nanohydroxyapatite composite. *Int. J. Nanomed.* **2015**, *10*, 1425–1447. [[CrossRef](#)]
81. Simões, I.G.; dos Reis, A.C.; da Costa Valente, M.L. Analysis of the influence of surface treatment by high-power laser irradiation on the surface properties of titanium dental implants: A systematic review. *J. Prosthet. Dent.* **2021**, 1–8, in press. [[CrossRef](#)]
82. Han, J.; Zhang, F.; Van Meerbeek, B.; Vleugels, J.; Braem, A.; Castagne, S. Laser surface texturing of zirconia-based ceramics for dental applications: A review. *Mater. Sci. Eng. C* **2021**, *123*, 112034. [[CrossRef](#)]
83. Cunha, A.; Oliveira, V.; Vilar, R. *Ultrafast Laser Surface Texturing of Titanium Alloys*; Elsevier Ltd.: Amsterdam, The Netherlands, 2016; ISBN 9780081009420.
84. Capellato, P.; Riedel, N.A.; Williams, J.D.; Machado, J.P.B.; Popat, K.C.; Claro, A.P.R.A. Surface Modification on Ti-30Ta Alloy for Biomedical Application. *Engineering* **2013**, *5*, 707–713. [[CrossRef](#)]
85. Luo, F.; Wang, L.; Xiao, Z.; Zhu, X.; Fan, Y.; Wang, K.; Zhang, X. Application of femtosecond laser microfabrication in the preparation of advanced bioactive titanium surfaces. *J. Mater. Chem. B* **2021**, *9*, 3912–3924. [[CrossRef](#)]
86. Muck, M.; Wolfsjäger, B.; Seibert, K.; Maier, C.; Lone, S.A.; Hassel, A.W.; Baumgartner, W.; Heitz, J. Femtosecond Laser-Processing of Pre-Anodized Ti-Based Bone Implants for Cell-Repellent Functionalization. *Nanomaterials* **2021**, *11*, 1342. [[CrossRef](#)] [[PubMed](#)]
87. Klos, A.; Sedao, X.; Itina, T.E.; Helfenstein-Didier, C.; Donnet, C.; Peyroche, S.; Vico, L.; Guignandon, A.; Dumas, V. Ultrafast Laser Processing of Nanostructured Patterns for the Control of Cell Adhesion and Migration on Titanium Alloy. *Nanomaterials* **2020**, *10*, 864. [[CrossRef](#)] [[PubMed](#)]

88. Bush, J.R.; Nayak, B.K.; Nair, L.S.; Gupta, M.C.; Laurencin, C.T. Improved bio-implant using ultrafast laser induced self-assembled nanotexture in titanium. *J. Biomed. Mater. Res. Part B Appl. Biomater.* **2011**, *97B*, 299–305. [[CrossRef](#)] [[PubMed](#)]
89. Liu, Y.; Rui, Z.; Cheng, W.; Song, L.; Xu, Y.; Li, R.; Zhang, X. Characterization and evaluation of a femtosecond laser-induced osseointegration and an anti-inflammatory structure generated on a titanium alloy. *Regen. Biomater.* **2021**, *8*, rbab006. [[CrossRef](#)]
90. Xie, H.; Zhang, C.; Wang, R.; Tang, H.; Mu, M.; Li, H.; Guo, Y.; Yang, L.; Tang, K. Femtosecond laser-induced periodic grooves and nanopore clusters make a synergistic effect on osteogenic differentiation. *Colloids Surf. B Biointerfaces* **2021**, *208*, 112021. [[CrossRef](#)]
91. Xie, D.; Xu, C.; Ye, C.; Mei, S.; Wang, L.; Zhu, Q.; Chen, Q.; Zhao, Q.; Xu, Z.; Wei, J.; et al. Fabrication of Submicro-Nano Structures on Polyetheretherketone Surface by Femtosecond Laser for Exciting Cellular Responses of MC3T3-E1 Cells/Gingival Epithelial Cells. *Int. J. Nanomed.* **2021**, *16*, 3201–3216. [[CrossRef](#)]
92. Daskalova, A.; Lasgorceix, M.; Bliznakova, I.; Angelova, L.; Hocquet, S.; Leriche, A.; Trifonov, A.; Buchvarov, I. Ultra-fast laser surface texturing of  $\beta$ -tricalcium phosphate ( $\beta$ -TCP) ceramics for bone-tissue engineering applications. *J. Phys. Conf. Ser.* **2020**, *1492*, 012059. [[CrossRef](#)]
93. Lasgorceix, M.; Ott, C.; Boilet, L.; Hocquet, S.; Leriche, A.; Asadian, M.; De Geyter, N.; Declercq, H.; Lardot, V.; Cambier, F. Micropatterning of beta tricalcium phosphate bioceramic surfaces, by femtosecond laser, for bone marrow stem cells behavior assessment. *Mater. Eng. C* **2019**, *95*, 371–380. [[CrossRef](#)]
94. Aivazi, M.; Fathi, M.H.; Nejatidanesh, F.; Mortazavi, V.; HashemiBeni, B.; Matinlinna, J.P.; Savabi, O. The evaluation of prepared microgroove pattern by femtosecond laser on alumina-zirconia nano-composite for endosseous dental implant application. *Lasers Med. Sci.* **2016**, *31*, 1837–1843. [[CrossRef](#)]
95. Sriramoju, V.; Alfano, R.R. In vivostudies of ultrafast near-infrared laser tissue bonding and wound healing. *J. Biomed. Opt.* **2015**, *20*, 108001. [[CrossRef](#)]
96. Amini-Nik, S.; Kraemer, D.; Cowan, M.L.; Gunaratne, K.; Nadesan, P.; Alman, B.A.; Miller, R.J.D. Ultrafast Mid-IR Laser Scalpel: Protein Signals of the Fundamental Limits to Minimally Invasive Surgery. *PLoS ONE* **2010**, *5*, e13053. [[CrossRef](#)] [[PubMed](#)]
97. Melvin, J.S.; Karthikeyan, T.; Cope, R.; Fehring, T.K. Early Failures in Total Hip Arthroplasty—A Changing Paradigm. *J. Arthroplast.* **2014**, *29*, 1285–1288. [[CrossRef](#)] [[PubMed](#)]
98. Dobzyniak, M.; Fehring, T.K.; Odum, S. Early Failure in Total Hip Arthroplasty. *Clin. Orthop. Relat. Res.* **2006**, *447*, 76–78. [[CrossRef](#)] [[PubMed](#)]
99. Pflüger, M.J.; Frömel, D.E.; Meurer, A. Total Hip Arthroplasty Revision Surgery: Impact of Morbidity on Perioperative Outcomes. *J. Arthroplast.* **2020**, *36*, 676–681. [[CrossRef](#)]
100. Hooper, J.; Schwarzkopf, R.; Fernandez, E.; Buckland, A.; Werner, J.; Einhorn, T.; Walker, P.S. Feasibility of single-use 3D-printed instruments for total knee arthroplasty. *Bone Jt. J.* **2010**, *101-B*, 115–120. [[CrossRef](#)]
101. Hasan, S.; van Hamersveld, K.T.; Marang-van de Mheen, P.J.; Kaptein, B.L.; Nelissen, R.G.H.H.; Toksvig-Larsen, S. Migration of a novel 3D-printed cementless versus a cemented total knee arthroplasty: Two-year results of a randomized controlled trial using radiostereometric analysis. *Bone Jt. J.* **2020**, *102-B*, 1016–1024. [[CrossRef](#)]
102. Mortini, P.; Boari, N.; Spina, A.; Bailo, M.; Franzin, A.; Gagliardi, F. The Suprameatal Dural Flap for Superior Petrosal Vein Protection during the Retrosigmoid Intradural Suprameatal Approach. *J. Neurol. Surg. Part A Cent. Eur. Neurosurg.* **2014**, *75*, 53–57. [[CrossRef](#)]
103. Neev, J.; Da Silva, L.B.; Feit, M.D.; Perry, M.D.; Rubenchik, A.M.; Stuart, B.C. Ultrashort pulse lasers for hard tissue ablation. *IEEE J. Sel. Top. Quantum Electron.* **1996**, *2*, 790–800. [[CrossRef](#)]
104. Ringer, A.J.; Bhamidipaty, S.V. Percutaneous Access to the Vertebral Bodies: A Video and Fluoroscopic Overview of Access Techniques for Trans-, Extra-, and Infrapedicular Approaches. *World Neurosurg.* **2013**, *80*, 428–435. [[CrossRef](#)]
105. Liu, X. A Novel Biportal Full Endoscopy Technique for Lumbar Lateral Recess Stenosis: Technical Report. *Clin. Spine Surg.* **2018**, *32*, 51–56. [[CrossRef](#)]
106. Kawamata, T.; Kamikawa, S.; Iseki, H.; Hori, T. Flexible Endoscope-Assisted Endonasal Transsphenoidal Surgery for Pituitary Tumors. *Min-Minim. Invasive Neurosurg.* **2002**, *45*, 208–210. [[CrossRef](#)] [[PubMed](#)]
107. Welcome, B.M.; Gilmer, B.B.; Lang, S.D.; Levitt, M.; Karch, M.M. Comparison of manual hand drill versus an electric dual-motor drill for bedside craniotomy. *Interdiscip. Neurosurg. Adv. Tech. Case Manag.* **2021**, *23*, 100928. [[CrossRef](#)]
108. Shin, B.J.; James, A.R.; Njoku, I.U.; Härtl, R. Pedicle screw navigation: A systematic review and meta-analysis of perforation risk for computer-navigated versus freehand insertion. *J. Neurosurg. Spine* **2012**, *17*, 113–122. [[CrossRef](#)] [[PubMed](#)]
109. Li, Z.; Yu, G.; Jiang, S.; Hu, L.; Li, W. Robot-assisted laminectomy in spinal surgery: A systematic review. *Ann. Transl. Med.* **2021**, *9*, 1–12. [[CrossRef](#)] [[PubMed](#)]